Hydroxypropyl methylcellulose hydrocolloid systems: Effect of hydroxypropy group content on the phase structure, rheological properties and film characteristics

Yanfei Wang[1,2], Jing Wang[1], Qingjie Sun[1,2], Xingfeng Xu[1,2], Man Li[1,2*], Fengwei Xie[3,†]

[1]*College of Food Science and Engineering, Qingdao Agricultural University, Qingdao, Shandong 266109, China*

[2]*Qingdao Special Food Research Institute, Qingdao, Shandong 266109, China*

[3]*International Institute for Nanocomposites Manufacturing (IINM), WMG, University of Warwick, Coventry CV4 7AL, United Kingdom*

*Corresponding author. *E-mail address*: manliqau@163.com (M. Li),

†Corresponding author. *E-mail addresses*: d.xie.2@warwick.ac.uk; fwhsieh@gmail.com (F. Xie)

Abstract

This work investigates the structure, processability, and film performance of hydroxypropyl methylcellulose (HPMC) hydrocolloids affected by hydroxypropy substitution degree and blending with hydroxypropyl starch (HPS). The hydroxypropylation of HPMC could increase inter-chain hydrogen bonding, thereby promoting its gelation, and improve film-forming, but reduce the mechanical properties of the films. HPMC-HPS mixed hydrocolloid system showed a typical "sea-island" morphology with the continuous phase changing with blend ratio. The content of hydroxypropy groups of HPMC affected the compatibility between HPMC and HPS, the morphology of the discrete phase, and the rheological properties of the blends. The fluid-like HPS enhanced the gel strength of HPMC when they had better compatibility. With a higher degree of hydroxypropy substitution, blend films exhibited a much denser structure, better oxygen barrier property, and appropriate mechanical properties. The knowledge obtained from this work could guide the development of edible packaging materials with desired properties and functionality.

Keywords: hydroxypropyl methylcellulose; hydroxypropyl starch; hydroxypropy group content; rheological properties; phase structure; oxygen barrier property

1 Introduction

Edible packaging based on natural polymers has been considered a promising alternative technology to traditional plastic packaging, which has attracted attention in recent years (Jeevahan et al., 2020; Mostafavi & Zaeim, 2020; Rangaraj, Rambabu, Banat, & Mittal, 2021). Although edible packaging cannot wholly replace petroleum-based plastic packaging, it may help to reduce the use of plastics, and thus alleviating plastic-related issues (Prabhu & Prashantha, 2018; Tavares, Souza, Goncalves, & Rocha, 2021; Zibaei et al., 2021). Edible packaging (films and coatings) can not only protect food from deterioration, but also be consumed directly along with the packed food products (Yong & Liu, 2021). Biopolymers, including polysaccharides and proteins, have been widely studied for the development of edible materials (Diaz-Montes & Castro-Munoz, 2021; Tavares et al., 2021).

Cellulose is the most abundant polysaccharide in nature. Hydroxypropyl methylcellulose (HPMC), a chemical derivative of cellulose with good water solubility and biodegradability and excellent film-forming capability, mechanical and barrier properties, has been widely applied in different applications such as edible packaging, medicinal capsules, and drug delivery systems (Lopez-Polo, Silva-Weiss, Zamorano, & Osorio, 2020). However, the high price (Allenspach, Timmins, Sharif, & Minko, 2020), high production energy consumption (Y. F. Wang, Yu, Sun, & Xie, 2021), and low oxygen-barrier property of HPMC (Ghadermazi, Hamdipour, Sadeghi, Ghadermazi, & Asl, 2019; Muhammad-Javeed & Mohammed, 2018) limit its broader applications largely. Regarding this, HPMC is often blended with other polymers to produce edible films, since blending different polymers has been considered as one of the most cost-effective methods to reduce costs, cope with the property limitations of pure polymer matrices, achieve enhanced and/or new material properties, and to expand applications (Aghjeh, Khonakdar, & Jafari, 2015; Gegenhuber, Krekhova, Schoebel, Groschel, & Schmalz, 2016). Hydroxypropyl starch (HPS) is an ideal material to be blended with HPMC because of its low cost, abundance, excellent gas barrier property, and wide application in the food industry (W. W. Wang, Sun, & Shi, 2019).

Thermodynamically, most polymer blends are immiscible or incompatible systems on the molecular scale (Ibrahim & Karrer, 2010). However, the compatibility between polymers plays a pivotal role in determining the morphology, processability and final properties of the blends (Tanaka, Sako, Hiraoka, Yamaguchi, & Yamaguchi, 2020). The degree of compatibility of polymer blends, on a larger scale, may vary to a great extent. HPMC should have good compatibility with HPS considering the same chemical repeat unit (glucose with hydroxyl groups) of both HPS and HPMC. However, HPMC dissolves in water at a low temperature and congeals at a high temperature (thermal gel), whereas HPS undergoes gelation on cooling but solates upon heating (cooling gel) (Polamaplly et al., 2019; Zhong, Xie, Zhang, Sun, Qi, & Li, 2020). The opposite temperature-induced gelation behaviors make it challenging to achieve a blend of these two biopolymers with high compatibility and fine phase distribution. Therefore, the compatibility and phase transition of HPMC-HPS blends are interesting scientifically and practically.

Cellulose is not soluble in usual solvents due to linear chains of D-glucose molecules linked by β-1,4-O bonds and hydrogen bonds between the chains, which limits its potential applications (S. Y. Li et al., 2020). However, with the replacement of hydroxyl groups by methoxy and hydroxypropoxy, cellulose turns into a water-soluble polysaccharide (Liang et al., 2018; Rangaraj et al., 2021). The degree of substitution (DS) with hydroxypropy groups and methoxy groups provide an operation window for adjusting the physical and chemical properties of HPMC, such as viscosity and gelling properties (Silva et al., 2021; Zhu et al., 2021).

In this study, edible films based on an HPMC-HPS hydrocolloid system were prepared by solution casting. While HPMC and HPS have similar chemical structures, our hypothesis is that the degree of hydroxypropylation of HPMC can affect the compatibility with HPS and the material structure and properties of HPMC-HPS blends. In contrast, most previous studies have focused on the effect of the DS of HPMC on emulsion-stabilization ability (Shimada, Fonseca, & Petri, 2017), hydration (Arai & Shikata, 2017), drug release performance (Caccavo, Lamberti, Barba, Abrahmsen-

Alami, Viriden, & Larsson, 2017), sewage treatment capacity (Martins, de Toledo, & Petri, 2017), and film properties (Otoni, Lorevice, de Moura, & Mattoso, 2018). Our results highlight largely the effect of the content of hydroxypropy groups in HPMC on the rheological properties, phase structure, and film properties of HPMC-HPS mixed hydrocolloid, which will guide the development of edible packaging materials with desired properties and functionality.

2 Materials and method

2.1 Materials

A food-grade hydroxypropylated high-amylose corn starch was supplied by Penford (Australia). Three commercially available pharmaceutical-grade HPMC products were purchased from Aladdin Biochemical Technology Co., Ltd (Shanghai, China), with specifications listed in **Table S1**. Poly(ethylene glycol) (PEG 400) with a weight-average molecular mass (M_w) of 400 was purchased from Sigma-Aldrich.

2.2 Preparation of HPMC-HPS solutions

HPMC-HPS solutions (8 wt%) with different ratios (10:0, 5:5, and 0:10, w/w) were prepared. Specifically, HPMC and HPS were mixed in a form of dry powder and then dispersed in hot water (70 °C) with stirring for 30 min. Afterwards, the suspensions were heated to 95 °C and maintained at this temperature for 1 h to gelatinize HPS in a water bath, which was then cooled down to room temperature to dissolve HPMC. Rheological measurements were then performed.

2.3 Film casting

Films were prepared with HPMC-HPS solutions of 5 wt% concentration added with 1.5% PEG as a plasticizer. Before film casting, solutions were kept at 70 °C for 40 min with slow stirring. To obtain films, solutions (20 g) were poured onto a Petri dish (15 cm diameter) and then dried at 37 °C, after which the dry films were peeled off from the dishes. All the films were then kept under 75%

relative humidity (RH) at 25 °C for at least 3 days for further characterization. The thicknesses of the blend films are listed in **Table S2**.

2.4 Rheological measurements

Dynamic rheological properties of samples were investigated using a strain-controlled rheometer (MCR302, Anton Paar, Austria). A parallel-plate geometry (50 mm diameter) with the gap set at 0.8 mm was used for the measurements.

To obtain the linear range of viscoelasticity, strain sweep measurements were performed from 0.01% to 100% at a frequency of 1 Hz at 25 °C.

Temperature sweeps involved heating from 5 °C to 85 °C at a heating rate of 2 °C/min. The frequency was set at 1 Hz and the strain at 1% (to be in the linear range of viscoelasticity). The sample was placed between the parallel plates, and then a small amount of silicone oil was applied to the periphery of the plates to prevent moisture evaporation.

Frequency sweeps from 1 rad/s to 100 rad/s were also performed after isothermal equilibration for 3 min at both 5 °C and 85 °C. The strain was set at 1% (to be in the linear range of viscoelasticity). Storage modulus (G'), loss modulus (G''), and tan δ were recorded. The frequency-dependence of G' and G'' can be shown in the following power-law equations:

$$G' = G'_0\omega^{n'} \quad (1)$$

$$G'' = G''_0\omega^{n''} \quad (2)$$

Based on these equations, the slopes (n' and n'') and intercepts (G_0' and G_0'') of log G' *vs.* log ω and log G'' *vs.* log ω can be calculated.

2.5 Light microscopy

HPMC-HPS (3:7, 5:5, and 7:3, w/w) solutions of a concentration of 3 wt% were used for microscopic observation with a Nikon Eclipse TE 2000-U optical microscope. The same method mentioned for solution preparation (**section 2.2**) was used to gelatinize HPS, and the solution was cooled down to 45 °C before casting on a glass. 1% (w/v) iodine alcohol solution, which was prepared by mixing 1 g of iodine and 10 g of potassium iodine solution in a 100mL flask, with ethanol subsequently added, was used to dye HPS. Afterwards, the films were dried at 45 °C before microscopic imaging.

2.6 Synchrotron small/wide-angle X-ray scattering (SAXS/WAXS)

SAXS/WAXS analyses of the films were carried out on the SAXS/WAXS beamline (flux, 10^{13} photons per second) at the Australian Synchrotron (Clayton, Vic, Australia) at a wavelength λ = 1.47 Å. The 2D scattering patterns were collected using a Pilatus 1M camera (active area, 169 × 179 mm; and pixel size, 172 × 172 μm). The scatterBrain software was used to acquire the one-dimensional (1D) data from the 2D scattering pattern. The SAXS data in the angular range of $0.015 < q < 0.15$ Å^{-1} and the WAXS data in the range of $0.095 < q < 2$ Å^{-1} were used, where $q = 4\pi\sin\theta/\lambda$, in which 2θ is the scattering angle and λ is the X-ray wavelength of the X-ray source. All data were background-subtracted, smeared-subtracted, and normalized before further analysis.

2.7 Mechanical properties

The mechanical properties of the films were measured according to the ASTM D5938 standard using an Instron tensile testing apparatus (5565). Tensile strength (σ_t), elongation at break (ε_b), and elastic modulus (E) were measured at a crosshead speed of 10 mm/min. For each sample, five specimens were tested.

2.8 Oxygen permeability (OP)

Oxygen transmission rates of the films (50 cm^2) were measured by Mocon OXTRAN® 2/21H Master (MH) and Satellite (SH) systems (Mocon Inc., Minneapolis, MN) according to the ASTM D-3985 standard.

2.9 Thermogravimetric analysis (TGA)

Thermogravimetric analysis (TGA) of the films was carried out using a TGA (PerkinElmer Pyris 1) system from 30 °C to 700 °C with a heating rate of 10 °C/min (in a nitrogen atmosphere).

3 Results and Discussions

3.1 Morphology of the HPMC-HPS blends

Since both HPMC and HPS are dissolvable in water but not soluble in ethanol, ethanol can be used as a solution for iodine to infuse and stain the materials without dissolving them (Y. F. Wang, Zhang, et al., 2016). **Fig. 1** shows the morphologies of HPMC-HPS blends with different HPMCs under optical microscopy. The blends displayed a typical "sea-island" structure, with the HPMC phase being bright while the HPS phase dark after being dyed with iodine. Clearly, the two polysaccharide phases were immiscible. As the ratio of HPMC increased from 50% to 70%, the continuous phase of the blend changed from HPS to HPMC.

For the blends with different HPMCs, the HPMC domains in an HPS matrix have different morphologies. With an increased DS of HPMC, the HPMC phase areas became larger, probably indicating reduced compatibility between the two polysaccharides.

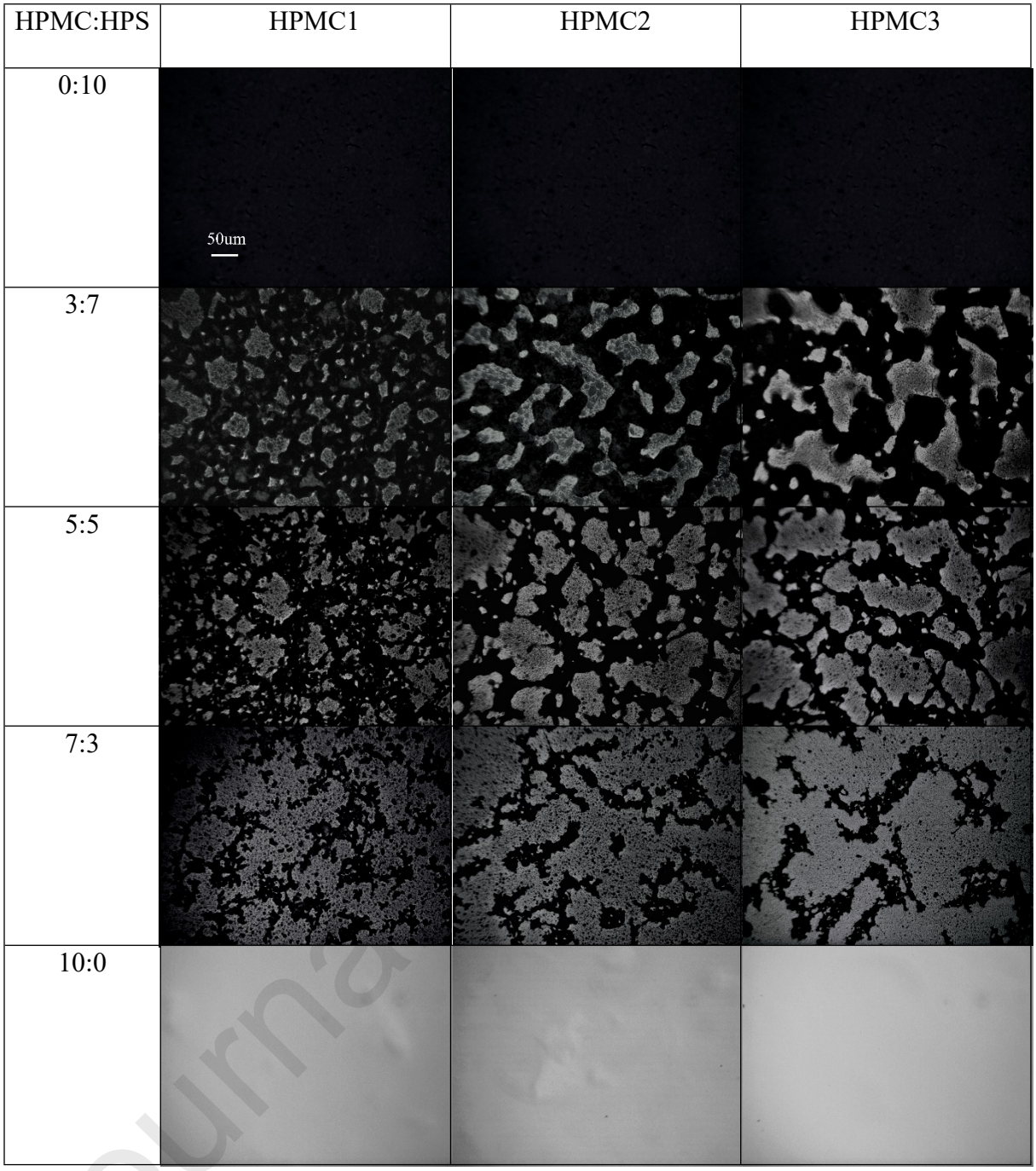

Fig. 1. Light microscopy images of HPMCs with different DSs, HPS and HPMC-HPS blends with the different HPMCs.

3.2 Rheological properties of the film-forming solutions

3.2.1 Linear viscoelastic regions

Strain sweep results (**Fig. S1**) indicate that, in the test range (0.01–100%), all the samples were solution ($G' < G''$) except for HPS ($G' > G''$). Besides, HPS showed an apparent decrease in G' and a remarkable increase in G'' when the strain was higher than 25%, whereas for the other samples both G' and G'' decreased at high strain. For HPMCs, the linear viscoelastic region was 0.01–40%. All HPMC-HPS blends were in a solution state at room temperature as only HPMCs. However, addition of HPS reduced the upper strain limit for linear viscoelasticity.

3.2.2 Viscoelastic property as a function of temperature

Fig. 2 shows the dynamic viscoelastic properties of HPMCs with different DSs, HPS, and HPMC-HPS blends with different HPMCs. For HPS, with the temperature increasing initially, G' was higher than G'', and both moduli decreased gradually, a common viscoelastic behavior of a gel. The cooling gelation of HPS had two distinct stages of the structural formation and the divide was the crossover of G' and G'' (*i.e.* the gel-sol transition at *ca.* 59 ℃). A higher temperature weakened starch chain interactions and increased chain mobility (Zhang et al., 2015).

For HPMCs, in the first temperature range, G' was below G'', and both moduli decreased more quickly than those of HPS with increasing temperature. Then, the structural formation of thermal gelation of HPMCs start with a sharp decrease in tan δ and divided into two stages by the crossover of G' and G'', which is consistent with other reports (Haque & Morris, 1993; Haque, Richardson, Morris, Gidley, & Caswell, 1993). The widely accepted mechanism is that HPMC chains existed in solution at low temperature with water cages surrounding hydrophobic clusters; heat absorbed first breaks the water cages and then exposes methyl groups to the aqueous surrounding; and then the hydrophobic association of hydrophobic groups on the polymer chains at higher temperatures led to a cross-linked network and gel formation.

HPS

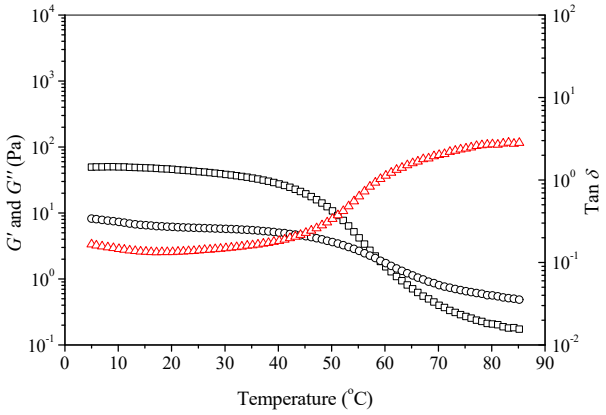

HPMC1

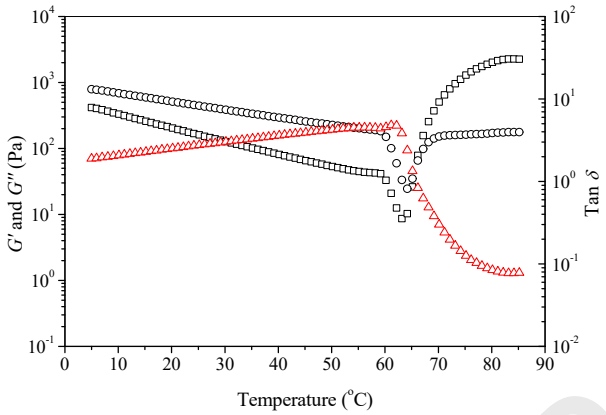

HPMC1-HPS

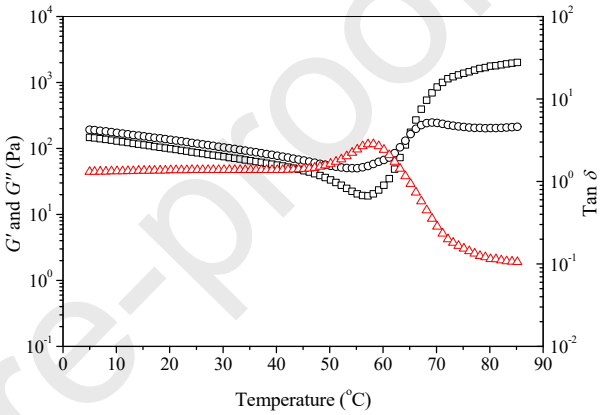

HPMC2

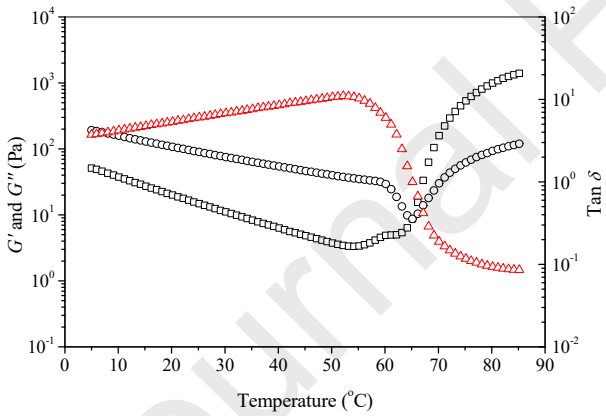

HPMC2-HPS

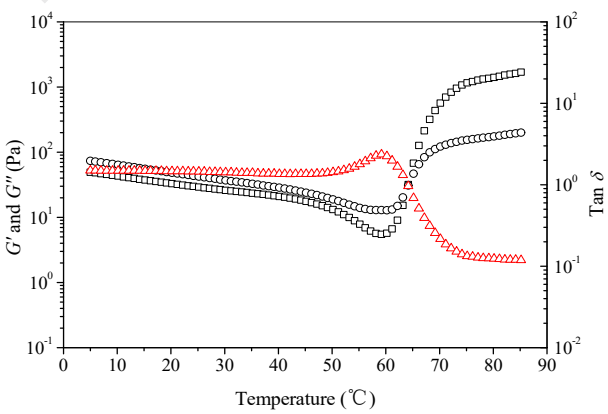

HPMC3

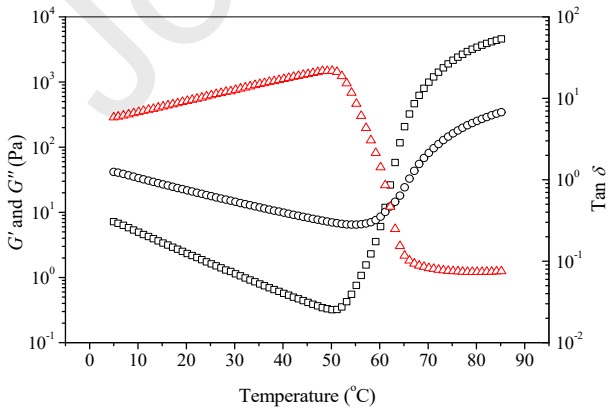

HPMC3-HPS

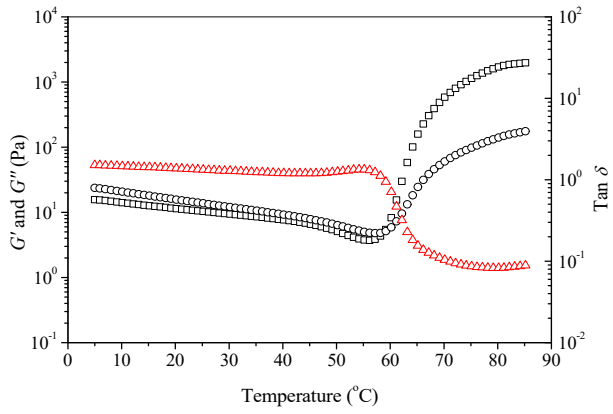

Fig. 2. Storage modulus (G', represented by square), loss modulus (G'', represented by triangle) and tanδ *vs.* temperature curves for the solutions of HPMCs with different DSs, HPS, and HPMC-HPS (5:5) blends with the different HPMCs.

It can be seen that for HPMC1, during the first stages of structural formation, G' and G'' decreased sharply with increasing temperature (62–65.8 ℃), as previously reported (Bajwa, Sammon, Timmins, & Melia, 2009). However, a higher DS could change the way the moduli change with temperature, and both moduli of HPMC3 increased with increasing temperature after 50 ℃. Moreover, the sol-gel transition shifted to a lower temperature with a higher DS. Specifically, the sol-gel transition temperatures of HPMC1, HPMC2, and HPMC3 were 65.8 ℃, 65.2 ℃, and 60.7 ℃, respectively. Regarding this, a higher DS results in higher inter-chain hydrogen bonding in HPMC, promoting gel structural formation.

For all the blends, the moduli increased with increasing temperature during the first stage of structural formation (57–64.8 ℃ for HPMC1-HPS, 59–64.1 ℃ for HPMC2-HPS, and 56–58.8 ℃ for HPMC3-HPS), indicating that HPS played an important role in the structural formation. The blends had intermediate moduli between those for individual HPMC and HPS. All the blends showed a similar pattern of viscoelastic properties to those for HPMCs due to the high viscosity of HPMC. However, blending HPMC with HPS made these effects of the DS of HPMC on G' and G'' less apparent. For the blends, tan δ showed a similar pattern to pure HPMCs, but showed a lower dependence on temperature at low temperatures.

3.2.3 Viscoelastic properties as a function of frequency

Fig. 3a and b shows the moduli (G' and G'') *vs.* frequency results at 5 °C for HPMCs with different DSs, HPS, and HPMC-HPS blends with different HPMCs. HPS showed a typical solid-like behavior ($G' > G''$), whereas all the HPMC samples were fluid-like ($G' < G''$). For the blends, G' was very close to G'', and in most of the test frequency range, G' was lower than G'', indicating a fluid-

like behavior. However, for HPMC1-HPS, the crossover of G' and G'' ($G' > G''$) occurred at a high frequency, and for HPMC3-HPS, this at a low frequency. This may be due to the incorporation of HPS, which was a gel at the test temperature (5 °C), into the liquid-like HPMCs.

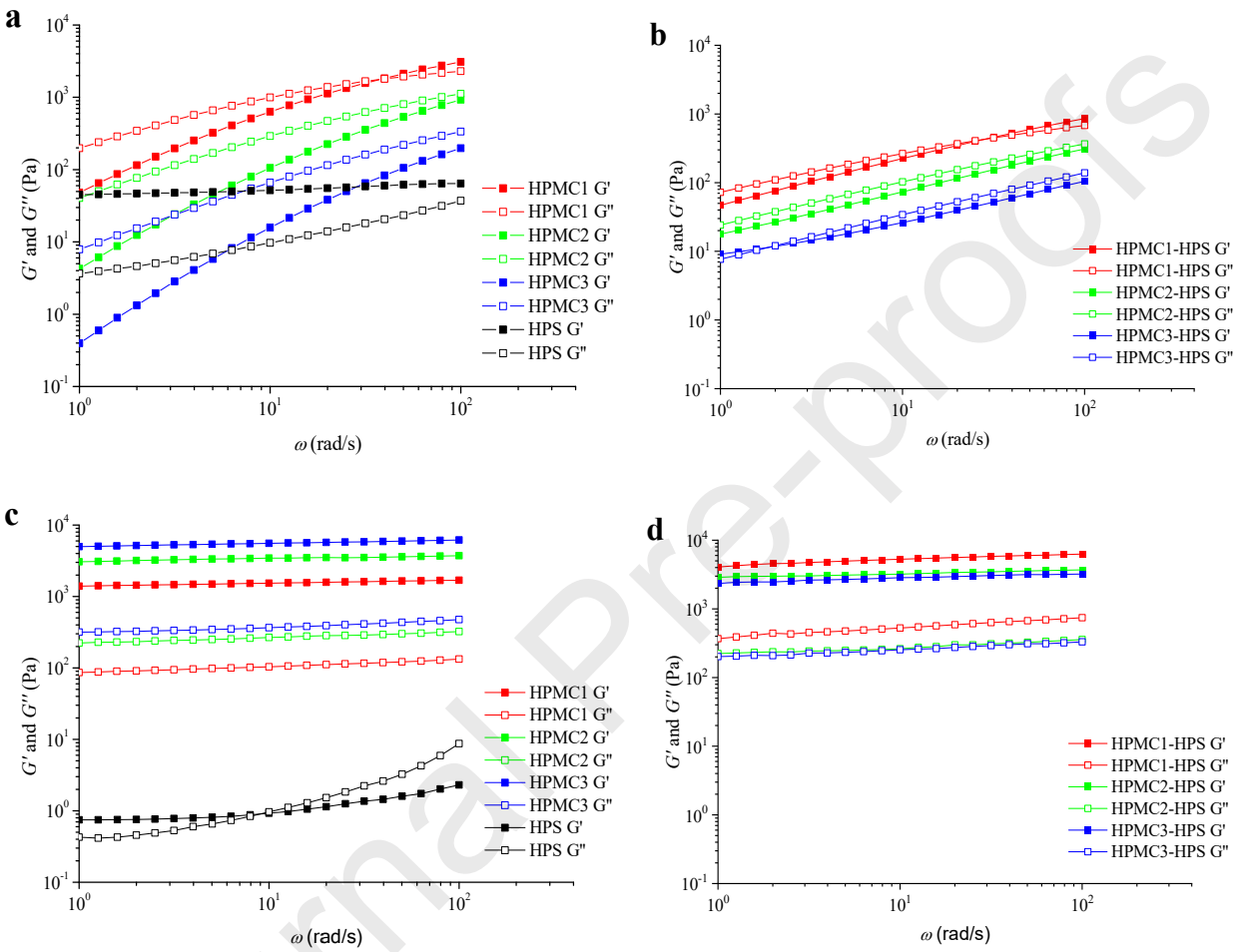

Fig. 3. Storage modulus (G') and loss modulus (G'') *vs.* frequency curves for HPMCs with different DSs, HPS, and HPMC-HPS (5:5) blends with the different HPMCs at 5 °C (a and b) and 85 °C (c and d).

Table S3 lists the n', n'', G_0' and G_0'' values for the different samples at 5 °C. HPS showed clearly a solid-like behavior since the slopes were close to 0, and G_0' was much higher than G_0'' (Ortega-Ojeda, Larsson, & Eliasson, 2004). For all the HPMCs, n' was close to 1, and G_0' was much lower than G_0'', confirming their liquid-like behavior (Zhang et al., 2015). For the blends, n' and n''

were slightly lower than those for HPMCs, suggesting that the blends behaved less like a liquid than HPMCs. HPMCs showed apparent frequency-dependence, whereas such dependence could hardly be observed for HPS. The blends also showed a frequency-dependence, which were slightly less apparent than that of HPMCs.

Both n' and n'' for HPMCs were increased with a higher DS, indicating that hydroxypropylation increased the liquid-like behavior of HPMC and the frequency-dependence at low temperatures. For the blends, with a higher DS of HPMC, n' was decreased, while n'' was increased, owing to the blending of HPS in a gel state. For both HPMCs and the blends, G_0' and G_0'' were decreased with an increased DS of HPMC, which may be attributed to the weakened viscoelasticity of HPMC as the main contributing component.

Fig. 3c and d shows that at 85 °C, HPMCs had a typical solid-like behavior with negligible frequency-dependence and $G' > G''$. For HPS, G' was lower than G'' at high frequency, indicating a liquid-like behavior, which corresponds to its liquid state at high temperature.

For HPMCs, a higher content of hydroxypropy groups led to increased moduli. In this regard, the increased number of hydroxypropy groups could promote chain interactions and facilitate gel formation. However, for the blends containing HPMC, the moduli decreased with a higher DS of HPMC, which could be due to decreased compatibility.

For all the blends, both n' and n'' were close to 0, and G_0' was much higher than G_0'' (**Table S3**), confirming their solid-like behavior at 85 °C. Besides, for the blends containing HPMC, both n' and n'' were close to those for HPMC, and the moduli remained stable with increasing frequency. All these results suggest that it was HPMC that mainly contributed to the viscoelasticity of the blend gels at a high temperature (85 °C).

The moduli of the blends containing HPMC2 or HPMC3 were between those of pure HPS and the respective pure HPMC. This could be due to the weakening effect of HPS, which is a solution at a high temperature. In contrast, for HPMC1, both G' and G'' of the blend were higher than those of

the pure HPMC. This may be attributed to the relatively good compatibility between HPMC1 and HPS.

3.3 Characteristics of films

3.3.1 Crystalline structure

Fig. S2a shows the SAXS patterns for the films of HPS and HPMCs. All the samples present apparent characteristic peaks at high q values ($q > 0.3$ Å^{-1}). From **Fig. S2a**, HPMCs showed a well-defined peak at about 0.537 Å^{-1}, indicating that all the HPMCs with different DSs have a certain crystalline structure. In contrast, HPS showed a well-defined peak at about 0.397 Å^{-1}, corresponding to the typical B-type crystalline structure of starch at 5.3°. With an increased content of hydroxypropy groups, the characteristic peak at 7.2° for HPMC seemed to be more intense. It is speculated that hydroxypropylation is favorable for cellulose processing (the disruption of the original hydrogen bonding network) and thus for post-processing recrystallization.

Fig. S2b shows the SAXS patterns for the HPMC-HPS blend films. All the blend samples showed two SAXS peaks at about 0.537 Å^{-1} and 0.397 Å^{-1}, corresponding to the characteristic peaks of HPMC (at 7.2°) and HPS (at 5.3°), respectively. As for pure HPMCs, the HPMC characteristic peak for the blends became more intense with an increased DS of HPMC. The intensity of the HPS characteristic peak at 5.3° did not show apparent change with variation in the DS of HPMC. Moreover, compared with for the corresponding pure samples, both the intensities of the HPMC and HPS characteristic peaks for the blends were smaller, indicating suppressed crystallization of both HPMC and HPS.

The crystallinity of polymer materials should largely influence their physical properties such as mechanical properties. These will be further discussed in the following sections.

3.3.2 Fractal structure

Fractal geometry is used to describe disordered objects possessing dilation symmetry, meaning that they look geometrically self-similar under the transformation of scale such as changing the magnification under microscopy (Schaefer, 1989). Fractal structures have two categories, namely mass fractal dimension (D_m) and surface fractal dimension (D_s), both of which can be calculated according to the Porod equation:

$$I(q) \propto q^{-\alpha} \qquad (3)$$

where I is the SAXS intensity, q is the scattering vector, and α is an exponent called the Porod slope (Suzuki, Chiba, & Yarno, 1997). The relation between α and D follows as $D_m = \alpha$ ($\alpha < 3$), and $D_s = 6 - \alpha$ ($3 < \alpha < 4$). D_m is used to indicate the compactness while D_s can be seen as an indicator of the degree of smoothness (Li, Wang, Zhao, Qiao, & Zhang, 2020).

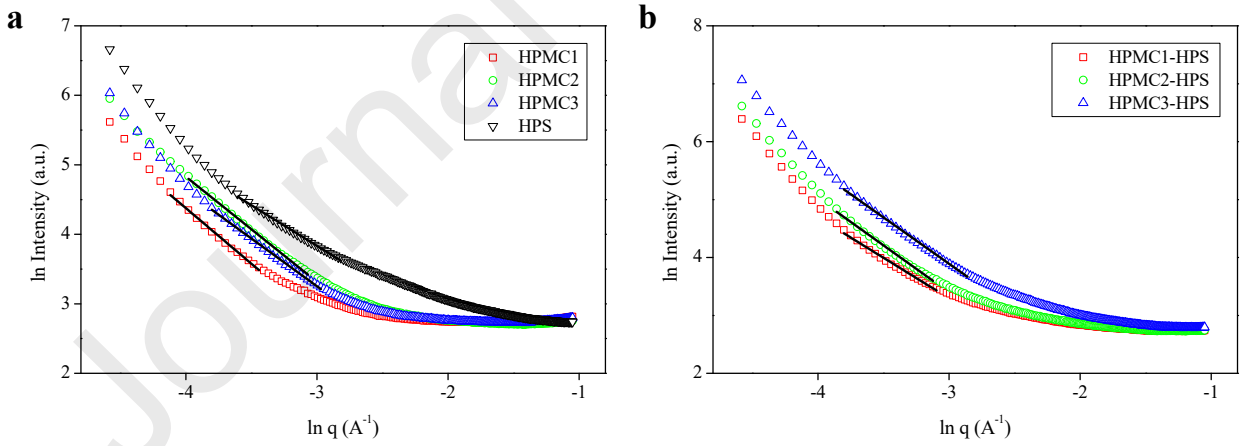

Fig. 4. ln$I(q)$ *vs.* ln$q$ patterns and their fitted curves for the films of HPMCs with different DSs, HPS, and HPMC-HPS (5:5) blends with the different HPMCs.

Fig. 4 shows the ln$I(q)$ *vs.* ln$q$ patterns and their fitted curves for HPMC-HPS blend films. All the samples were seen to have a self-similar fractal structure within a certain limit. Since all the Porod

slopes (α) were smaller than 3, the fractal structures in all the samples were presented as a mass fractal, indicating HPMC-HPS films had a smooth surface with the fractal dimension $D = D_m = \alpha$. The fractal structure parameters for HPMC-HPS blend films were provided in **Table S4**. Concerning pure HPMC, the D value for HPMC1 was the largest, and with an increased DS, the D value for HPMC decreased gradually, indicating that the incorporation of bulky hydroxypropy groups in methylcellulose molecules led to a self-similar structure with a lower density.

For the 5:5 HPMC-HPS blend, the D value increased with a higher DS of HPMC, which might result from the decreased compatibility between HPMC and HPS. A similar result was shown in HPMC-HPS with different molar substitution with hydroxypropy groups in HPS (Y. F. Wang et al., 2018).

3.3.3 Tensile properties

The E, σ_t and ε_b values of HPMC-HPS films were shown in **Fig. 7**. For pure HPMC films, a higher DS of HPMC generally led to lower E, σ_t, and ε_b, indicating that the hydroxypropylation of HPMC decreased material mechanical properties probably by reducing chain interactions (hydrogen bonding) after cooling.

With a higher DS, the E, σ_t and ε_b values of the blends were reduced, which corresponds to the reduced compatibility between HPS and HPMC. The σ_t values of the blend samples were between those of the two single-polymer films, but closer to that of HPS. The E values of the blend samples were close to that of HPMC, but the E values of HPMC1-HPS were higher than those of the two pure components. This could be due to the good compatibility between HPMC1 and HPS as shown in microscopy results. The blends with HPMC2 or HPMC3 even showed lower ε_b values than that of either HPMC or HPS, indicating reduced compatibility between the two biopolymers at a high DS of HPMC. Incompatible polymers have a phase-separated structure and tend to form weak points, which are detrimental to stress transfer.

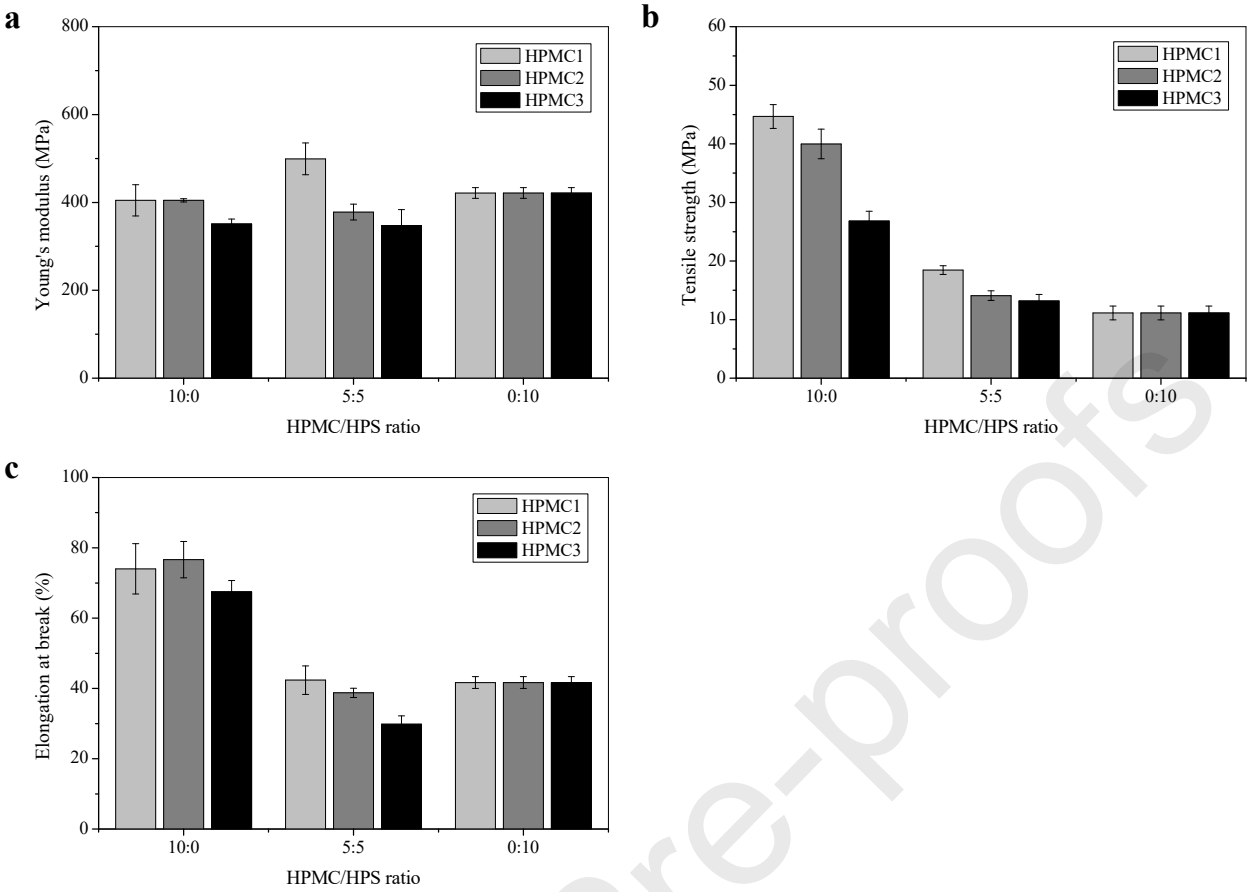

Fig. 5. Tensile properties of the films of HPMCs with different DSs, HPS, and HPMC-HPS (5:5) blends with the different HPMCs.

For both pure HPMCs and HPMC-HPS blends, a high DS of HPMC led to marginally higher crystallinity (see the SAXS results) but decreased mechanical properties. This indicates the mechanical properties were mainly determined by chain interactions (hydrogen bonding).

3.3.4 Oxygen permeability

The oxygen permeability (OP) results of HPMC-HPS films were shown in **Fig. 6**. The OP values of pure HPMC films were all much higher than that of the pure HPS film, indicating the better oxygen barrier property of starch films (Ortega-Toro, Jimenez, Talens, & Chiralt, 2014; Y. F. Wang, Yu, et al., 2016). For pure HPMC films, an increased content of hydroxypropy groups resulted in a decrease in OP, which could be ascribed to reduced chain interactions.

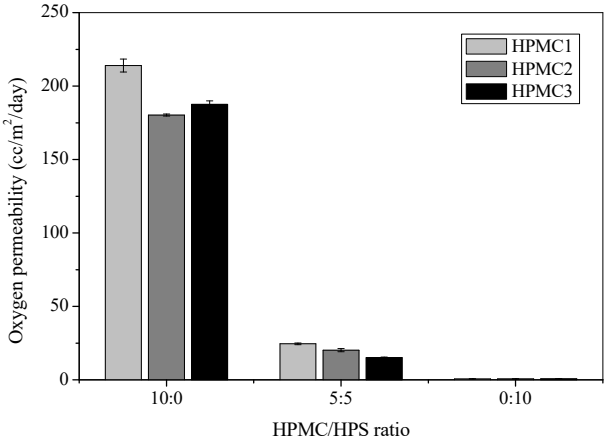

Fig. 6. Oxygen permeability of the films of HPMCs with different DSs, HPS, and HPMC-HPS (5:5) blends with the different HPMCs.

For the blend films, with an increased content of HPS, the OP value of films decreased considerably, which is in agreement with our previous study (Y. F. Wang, Yu, et al., 2016). Besides, the OP value decreased with an increased DS of HPMC (similar to that of pure HPMC films), indicating the hydroxypropy groups content of HPMC had a significant effect on the OP value although HPS plays a much more important role in the OP of the blends. This also suggests that OP is mainly determined by the chemical nature of polysaccharides but not the density of the self-similar structure.

3.3.5 Thermal degradation

The TGA and DTG (derivative thermogravimetric analysis) curves for the films (see **Fig. S3**) show two well defined thermal degradation stages. The first stage took place between 30 and 180 °C, which can be attributed to the moisture evaporation from the materials. The second stage related to the thermal decomposition of the polysaccharides occurred in the temperature range of 300–450 °C. Pure HPMC films displayed a similar peak at 361 °C, while the pure HPS film showed lower thermal stability, with its decomposition occurring at 315 °C. All the blend samples showed two

decomposition peaks at 361 °C and 312 °C, representing HPMC and HPS respectively, implying that the content of hydroxypropyl groups in HPMC did not affect the thermal stability of the blends.

3.4 Further discussion

It is known that a small change in the chemical structure of polymers can result in dramatic changes in their rheological properties (Chun & Yoo, 2007). In turn, the understanding of changes in the rheological properties of polymers caused by chemical modification is helpful in understanding their structure and other properties (Lee & Yoo, 2011). In this study, the rheological properties of polysaccharide solutions show an obvious dependence on the DS of HPMC. Although a higher content of hydroxypropy groups led to increased moduli of HPMC, the moduli of the blends decreased with a higher DS of HPMC, which means HPS disrupted the hydrophobic interactions and thus the gelation of HPMC at a high temperature. The moduli of HPMC1-HPS at 85 °C were higher than that of the two pure components. This indicates better compatibility between HPMC1 and HPS, which is also confirmed by the morphology results and tensile mechanical properties.

While the influence of cellulose hydroxypropylation on the crystallinity and factual structure of pure HPMCs and HPMC-HPS blend films was noticed, our data indicate the film physical properties (mechanical properties, OP, and thermal stability) were not mainly determined by crystallinity and the density of the self-similar structure, but rather by the chemical nature of polysaccharides and their chain interactions.

4 Conclusion

This work concerns the effect of hydroxypropylation of HPMC and blending with HPS on the structure, rheological properties, and film performance of HPMC hydrocolloids. HPMC-HPS mixed hydrocolloid systems showed a typical “sea-island” morphology with the continuous phase changing

with blend ratio. With a higher DS of HPMC, the HPMC domains in the HPS matrix become more combined leading to larger areas, suggesting reduced compatibility between the two polysaccharides.

HPMC played a dominant role in the rheological properties of HPMC-HPS blends. A higher DS of HPMC led to a decreased gelling temperature and an increased gel strength. Regarding this, the incorporation of hydroxypropy groups increased the inter-chain hydrophobic interactions of HPMC at a high temperature, and thereby promoting the thermal gelation of HPMC. The compatibility between HPMC and HPS decreased with a higher DS of HPMC. Interestingly, at a high temperature, the liquid-like HPS could enhance the gel strength of HPMC when they had good compatibility.

The content hydroxypropy groups in HPMC influenced the crystallinity, fractal structure, OP, and mechanical properties of HPMC-HPS blend films. A higher DS caused greater compactness of the self-similar structure as reflected by higher *D*. An increase in the DS of HPMC led to higher crystallinity and reduced OP. The mechanical properties of the blends were generally between those of the individual polysaccharides, while a higher DS of HPMC decreased the mechanical properties of both pure HPMCs and the HPMC-HPS blends.

Our results here have shown that the structure and properties of HPMC-HPS biphasic systems could be changed by the chemical modification of cellulose. Based on the results of this work, appropriate chemically modified HPMC and starch could be selected to develop new materials for food packaging and even wider applications.

Acknowledgements

This work was financially supported by the Doctoral Foundation of Qingdao Agricultural University (6631120081), the Program for Youth Science Innovation in Colleges and Universities in Shandong Province (2020KJF005), the Special Funds for Taishan Scholars Projects of Shandong Province (201712058), and the Research Fund of Qingdao Special Food Research Institute

(66120008). Part of this research was undertaken on the SAXS/WAXS beamline at the Australian Synchrotron, Victoria, Australia.

Conflicts of interest

There are no conflicts of interest to declare.

Reference

Uncategorized References

Aghjeh, M. R., Khonakdar, H. A., & Jafari, S. H. (2015). Application of mean-field theory in PP/EVA blends by focusing on dynamic mechanical properties in correlation with miscibility analysis. *Composites Part B, 79*, 74-82.

Allenspach, C., Timmins, P., Sharif, S., & Minko, T. (2020). Characterization of a novel hydroxypropyl methylcellulose (HPMC) direct compression grade excipient for pharmaceutical tablets. *International Journal of Pharmaceutics, 583*. https://doi.org/10.1016/j.ijpharm.2020.119343.

Arai, K., & Shikata, T. (2017). Hydration/Dehydration Behavior of Cellulose Ethers in Aqueous Solution. *Macromolecules, 50*(15), 5920-5928. https://doi.org/10.1021/acs.macromol.7b00848.

Bajwa, G. S., Sammon, C., Timmins, P., & Melia, C. D. (2009). Molecular and mechanical properties of hydroxypropyl methylcellulose solutions during the sol:gel transition. *Polymer, 50*(19), 4571-4576.

Caccavo, D., Lamberti, G., Barba, A. A., Abrahmsen-Alami, S., Viriden, A., & Larsson, A. (2017). Effects of HPMC substituent pattern on water up-take, polymer and drug release: An experimental and modelling study. *International Journal of Pharmaceutics, 528*(1-2), 705-713. https://doi.org/10.1016/j.ijpharm.2017.06.064.

Chun, S. Y., & Yoo, B. (2007). Effect of Molar Substitution on Rheological Properties of Hydroxypropylated Rice Starch Pastes. *Starch - Starke, 59*(7), 334-341.

Diaz-Montes, E., & Castro-Munoz, R. (2021). Edible Films and Coatings as Food-Quality Preservers: An Overview. *Foods, 10*(2), 249. https://doi.org/10.3390/foods10020249.

Gegenhuber, T., Krekhova, M., Schoebel, J., Groschel, A. H., & Schmalz, H. (2016). "Patchy" Carbon Nanotubes as Efficient Compatibilizers for Polymer Blends. *Acs Macro Letters, 5*(3), 306-310.

Ghadermazi, R., Hamdipour, S., Sadeghi, K., Ghadermazi, R., & Asl, A. K. (2019). Effect of various additives on the properties of the films and coatings derived from hydroxypropyl methylcellulose-A review. *Food Science & Nutrition, 7*(11), 3363-3377. https://doi.org/10.1002/fsn3.1206.

Haque, A., & Morris, E. R. (1993). Thermogelation of methylcellulose .1. Molecular-structures and processes. *Carbohydrate Polymers, 22*(3), 161-173. https://doi.org/10.1016/0144-8617(93)90137-S.

Haque, A., Richardson, R. K., Morris, E. R., Gidley, M. J., & Caswell, D. C. (1993). Thermogelation of methylcellulose .2. Effect of hydroxypropyl substituents. *Carbohydrate Polymers, 22*(3), 175-186. https://doi.org/10.1016/0144-8617(93)90138-T.

Ibrahim, B. A., & Karrer, M. K. (2010). Influence of Polymer Blending on Mechanical and Thermal Properties. *Modern Applied Science, 4*(9), 157-161.

Jeevahan, J. J., Chandrasekaran, M., Venkatesan, S. P., Sriram, V., Joseph, G. B., Mageshwaran, G., & Durairaj, R. B. (2020). Scaling up difficulties and commercial aspects of edible films for food packaging: A review. *Trends in Food Science & Technology, 100*, 210-222. https://doi.org/10.1016/j.tifs.2020.04.014.

Lee, H. L., & Yoo, B. (2011). Effect of hydroxypropylation on physical and rheological properties of sweet potato starch. *LWT - Food Science and Technology, 44*(3), 765-770.

Li, N., Wang, L., Zhao, S., Qiao, D., & Zhang, B. (2020). An insight into starch slowly digestible features enhanced by microwave treatment. *Food Hydrocolloids, 103*, 105690.

Li, S. Y., Ma, Y. L., Ji, T. T., Sameen, D. E., Ahmed, S., Qin, W., . . . Liu, Y. W. (2020). Cassava starch/carboxymethylcellulose edible films embedded with lactic acid bacteria to extend the shelf life of banana. *Carbohydrate Polymers, 248*, 116805. https://doi.org/10.1016/j.carbpol.2020.116805.

Liang, Z., Xfw, A., Hl, B., Long, Y. B., Yw, B., Gps, C., & Jq, A. (2018). Effect of plasticizers on microstructure, compatibility and mechanical property of hydroxypropyl methylcellulose/hydroxypropyl starch blends - ScienceDirect. *International Journal of Biological Macromolecules, 119*, 141-148.

Lopez-Polo, J., Silva-Weiss, A., Zamorano, M., & Osorio, F. A. (2020). Humectability and physical properties of hydroxypropyl methylcellulose coatings with liposome-cellulose nanofibers: Food application. *Carbohydrate Polymers, 231*, 115702. https://doi.org/10.1016/j.carbpol.2019.115702.

Martins, B. F., de Toledo, P. V. O., & Petri, D. F. S. (2017). Hydroxypropyl methylcellulose based aerogels: Synthesis, characterization and application as adsorbents for wastewater pollutants. *Carbohydrate Polymers, 155*, 173-181. https://doi.org/10.1016/j.carbpol.2016.08.082.

Mostafavi, F. S., & Zaeim, D. (2020). Agar-based edible films for food packaging applications - A review. *International Journal of Biological Macromolecules, 159*, 1165-1176. https://doi.org/10.1016/j.ijbiomac.2020.05.123.

Muhammad-Javeed, A., & Mohammed, A. (2018). Study of the barrier and mechanical properties of packaging edible films fabricated with hydroxypropyl methylcellulose (HPMC) combined with electro-activated whey. *Journal of Packaging Technology and Research, 2*, 169-180.

Ortega-Ojeda, F. E., Larsson, H., & Eliasson, A. C. (2004). Gel formation in mixtures of amylose and high amylopectin potato starch. *Carbohydrate Polymers, 57*(1), 55-66. https://doi.org/10.1016/j.carbpol.2004.03.024.

Ortega-Toro, R., Jimenez, A., Talens, P., & Chiralt, A. (2014). Properties of starch-hydroxypropyl methylcellulose based films obtained by compression molding. *Carbohydrate Polymers, 109*, 155-165. https://doi.org/10.1016/j.carbpol.2014.03.059.

Otoni, C. G., Lorevice, M. V., de Moura, M. R., & Mattoso, L. H. C. (2018). On the effects of hydroxyl substitution degree and molecular weight on mechanical and water barrier properties of hydroxypropyl methylcellulose films. *Carbohydrate Polymers, 185*, 105-111. https://doi.org/10.1016/j.carbpol.2018.01.016.

Polamaplly, P., Cheng, Y. L., Shi, X. L., Manikandan, K., Zhang, X., Kremer, G. E., & Qin, H. T. (2019). 3D printing and characterization of hydroxypropyl methylcellulose and methylcellulose for biodegradable support structures. *Polymer, 173*, 119-126. https://doi.org/10.1016/j.polymer.2019.04.013.

Prabhu, T. N., & Prashantha, K. (2018). A Review on Present Status and Future Challenges of Starch Based Polymer Films and Their Composites in Food Packaging Applications. *Polymer Composites, 39*(7), 2499-2522. https://doi.org/10.1002/pc.24236.

Rangaraj, V. M., Rambabu, K., Banat, F., & Mittal, V. (2021). Natural antioxidants-based edible active food packaging: An overview of current advancements. *Food Bioscience, 43*. https://doi.org/10.1016/j.fbio.2021.101251.

Schaefer, D. W. (1989). Polymers, fractals, and ceramic materials. *Science, 243*(4894), 1023-1027.

Shimada, R. T., Fonseca, M. S., & Petri, D. F. S. (2017). The role of hydroxypropyl methylcellulose structural parameters on the stability of emulsions containing Spirulina biomass. *Colloids and Surfaces a-Physicochemical and Engineering Aspects, 529*, 137-145. https://doi.org/10.1016/j.colsurfa.2017.06.001.

Silva, P. M., Prieto, C., Lagaron, J. M., Pastrana, L. M., Coimbra, M. A., Vicente, A. A., & Cerqueira, M. A. (2021). Food-grade hydroxypropyl methylcellulose-based formulations for electrohydrodynamic processing: Part I & ndash; Role of solution parameters on fibre and particle production. *Food Hydrocolloids, 118*, 106761. https://doi.org/10.1016/j.foodhyd.2021.106761.

Suzuki, T., Chiba, A., & Yarno, T. (1997). Interpretation of small angle x-ray scattering from starch on the basis of fractals. *Carbohydrate Polymers, 34*(4), 357-363.

Tanaka, Y., Sako, T., Hiraoka, T., Yamaguchi, M., & Yamaguchi, M. (2020). Effect of morphology on shear viscosity for binary blends of polycarbonate and polystyrene. *Journal of Applied Polymer Science, 137*(46), 49516.

Tavares, L., Souza, H. K. S., Goncalves, M. P., & Rocha, C. M. R. (2021). Physicochemical and microstructural properties of composite edible film obtained by complex coacervation between chitosan and whey protein isolate. *Food Hydrocolloids, 113*, 1064741. https://doi.org/10.1016/j.foodhyd.2020.106471.

Wang, W. W., Sun, Z. H., & Shi, Y. C. (2019). An improved method to determine the hydroxypropyl content in modified starches by H-1 NMR. *Food Chemistry, 295*, 556-562. https://doi.org/10.1016/j.foodchem.2019.05.152.

Wang, Y. F., Yu, L., Sun, Q. J., & Xie, F. W. (2021). Hydroxypropyl methylcellulose and hydroxypropyl starch: Rheological and gelation effects on the phase structure of their mixed hydrocolloid system. *Food Hydrocolloids, 115*, 106598. https://doi.org/10.1016/j.foodhyd.2021.106598.

Wang, Y. F., Yu, L., Xie, F. W., Li, S., Sun, Q. J., Liu, H. S., & Chen, L. (2018). On the investigation of thermal/cooling-gel biphasic systems based on hydroxypropyl methylcellulose and hydroxypropyl starch. *Industrial Crops and Products, 124*, 418-428. https://doi.org/10.1016/j.indcrop.2018.08.010.

Wang, Y. F., Yu, L., Xie, F. W., Zhang, L., Liao, L., Liu, H. S., & Chen, L. (2016). Morphology and properties of thermal/cooling-gel bi-phasic systems based on hydroxypropyl methylcellulose and hydroxypropyl starch. *Composites Part B-Engineering, 101*, 46-52. https://doi.org/10.1016/j.compositesb.2016.06.081.

Wang, Y. F., Zhang, L., Liu, H. S., Yu, L., Simon, G. P., Zhang, N. Z., & Chen, L. (2016). Relationship between morphologies and mechanical properties of hydroxypropyl methylcellulose/hydroxypropyl starch blends. *Carbohydrate Polymers, 153*, 329-335. https://doi.org/10.1016/j.carbpol.2016.07.029.

Yong, H. M., & Liu, J. (2021). Active packaging films and edible coatings based on polyphenol-rich propolis extract: A review. *Comprehensive Reviews in Food Science and Food Safety, 20*(2), 2106-2145. https://doi.org/10.1111/1541-4337.12697.

Zhang, L., Wang, Y. F., Yu, L., Liu, H. S., Simon, G., Zhang, N. Z., & Chen, L. (2015). Rheological and gel properties of hydroxypropyl methylcellulose/hydroxypropyl starch blends. *Colloid and Polymer Science, 293*(1), 229-237. https://doi.org/10.1007/s00396-014-3407-5.

Zhong, M. M., Xie, F. Y., Zhang, S., Sun, Y. F., Qi, B. K., & Li, Y. (2020). Preparation and digestive characteristics of a novel soybean lipophilic protein-hydroxypropyl methylcellulose-calcium chloride thermosensitive emulsion gel. *Food Hydrocolloids, 106*, 105891. https://doi.org/10.1016/j.foodhyd.2020.105891.

Zhu, J. S., Qian, Z. J., Eid, M., Zhan, F. C., Ismail, M. A., Li, J., & Li, B. (2021). Foaming and rheological properties of hydroxypropyl methylcellulose and welan gum composite system: The stabilizing mechanism. *Food Hydrocolloids, 112*, 106275. https://doi.org/10.1016/j.foodhyd.2020.106275.

Zibaei, R., Hasanvand, S., Hashami, Z., Roshandel, Z., Rouhi, M., Guimaraes, J. D., . . . Mohammadi, R. (2021). Applications of emerging botanical hydrocolloids for edible films: A review. *Carbohydrate Polymers, 256*, 117554. https://doi.org/10.1016/j.carbpol.2020.117554.

CRediT author statement:

Yanfei Wang: Conceptualization, Methodology, Investigation, Data Curation, Validation, Formal analysis, Writing - Original Draft, Visualization, Supervision. **Jing Wang**: Methodology, Investigation, Data Curation, Validation, Formal analysis. **Qingjie Sun:** Methodology, Resources. **Xingfeng Xu:** Methodology, Resources. **Man Li:** Methodology, Resources, Project administration, Funding acquisition, Supervision. **Fengwei Xie**: Conceptualisation, Methodology, Resources, Writing - Review & Editing, Visualization.

Highlights:

- ✓ Hydroxypropyl methylcellulose (HPMC) was blended with hydroxypropyl starch (HPS)
- ✓ The continuous phase of HPMC-HPS mixed hydrocolloid changed with HPMC/HPS ratio
- ✓ Hydroxypropylation promoted HPMC gelation
- ✓ Good compatibility between HPMC and HPS enhanced the HPMC-HPS gel strength
- ✓ HPMC hydroxypropylation improved the oxygen barrier effect of HPMC-HPS film